Journal of Organometallic Chemistry 927 (2020) 121544

Contents lists available at ScienceDirect

Journal of Organometallic Chemistry

journal homepage: www.elsevier.com/locate/jorganchem

Synthesis and characterization of *N*-(arylmethylene)-benzimidazole/imidazole-borane compounds

Wei-Ming Liu, Min Zhang, Jian-Feng Yan, Cai-Xia Lin*, Yao-Feng Yuan*

Key Laboratory of Molecule Synthesis and Function Discovery (Fujian Province University), Department of Chemistry, Fuzhou University, Fuzhou 350108, People's Republic of China

ARTICLE INFO

Article history:
Received 25 February 2020
Revised 15 September 2020
Accepted 21 September 2020
Available online 2 October 2020

Keywords:
Ferrocene
Imidazole
Borane
Thermal properties
Combustion test;Catalytic effect on ammonium perchlorate

ABSTRACT

N-(arylmethylene)-benzimidazole/imidazole-borane compounds (**7-10**) based on ferrocene/benzene were synthesized in a cost-effective way by reacting *N*-(arylmethylene)-benzimidazole/imidazoles with ammonium sulfate ($(NH_4)_2SO_4$) and sodium borohydride ($NaBH_4$). The structures of compounds **7-9** were determined by X-ray crystallography. Four compounds displayed high thermal decomposition temperatures (182-256°C) according to the thermogravimetry (TG) measurements. Interestingly, these compounds showed promising applications as potential propellant due to their spontaneous combustion upon contact concentrated HNO_3 (≥ 95 %) and catalytic effect on the thermal degradation of ammonium perchlorate (AP).

1. Introduction

It is well known that ferrocene derivatives are a kind of important burning rate catalysts (BRCs) of composite solid rocket propellants [1,2]. Most of them have catalytic effects on ammonium perchlorate (AP), which is known as one of the most common oxidizer in composite solid rocket propellants. Ferrocenyl nitrogen heterocyclic compounds [3–6] are representative type of these derivatives due to their low volatility [7], microscopic homogeneities in distribution [8], higher compatibility with organic binders [9], broad range of burning rate adjustments [10–12] and excellent ignition performance. In the past decade, it had been found that imidazolium borohydride [13–16], *N*-alkylimidazole-borane adducts [17] and imidazolyl-amine-BH_2 [18] were promising green propellants for future space propulsion. Imidazole-borane compounds that contained B-H bonds showed excellent integrated properties and ignition performances [19]. Thus, it would be an interesting research topic to study the burning rate catalytic performance of compounds containing both ferrocene and imidazole-borane groups. Nevertheless, ferrocene derivatives of imidazole-borane as potentially BRCs have been rarely reported so far. Herein, in this work *N*-(ferrocenylmethyl)-benzimidazole-borane (**7**) and *N*-(ferrocenylmethyl)- imidazole-borane (**8**) were synthesized and *N*-(benzyl)-benzimidazole-borane (**9**) and *N*-(benzyl)-imidazole-borane (**10**) were also prepared for comparation. In additon, compounds **7-9** were characterized by X-ray crystallography. The compounds showed promising applications as potential propellant due to their spontaneous combustion upon contact concentrated HNO_3 (≥ 95 %) and effectively accelerated the thermal degradation of AP.

2. Results and discussion

2.1. Synthesis

As depicted in Scheme 1, using ferrocenyl quaternary ammonium salt (**1**) or benzyl bromide (**2**) as raw materials, the intermediate compounds **3-6** were obtained by reacted with imidazole/benzimidazole respectively. Then these intermediates were reacted with $NaBH_4$ and $(NH_4)_2SO_4$ in anhydrous THF to give products **7-10**. Among them, compound **10** had been reported in literature without the relevant thermal property experiments [25].

2.2. Crystal structures

To gain insight into the structural characteristics of imidazole-borane adducts, the crystals of compounds **7-9** were obtained by slow diffusion of petroleum ether into the dichloromethane solution of them. The spatial structures of them were confirmed by X-ray crystallography. The crystallographic data and collection were summarized in Table 1. Selected bonds distances and angles were given in Tables S1-S6.

* Correspondence author.
E-mail address: yaofeng_yuan@fzu.edu.cn (Y.-F. Yuan).

https://doi.org/10.1016/j.jorganchem.2020.121544
0022-328X/

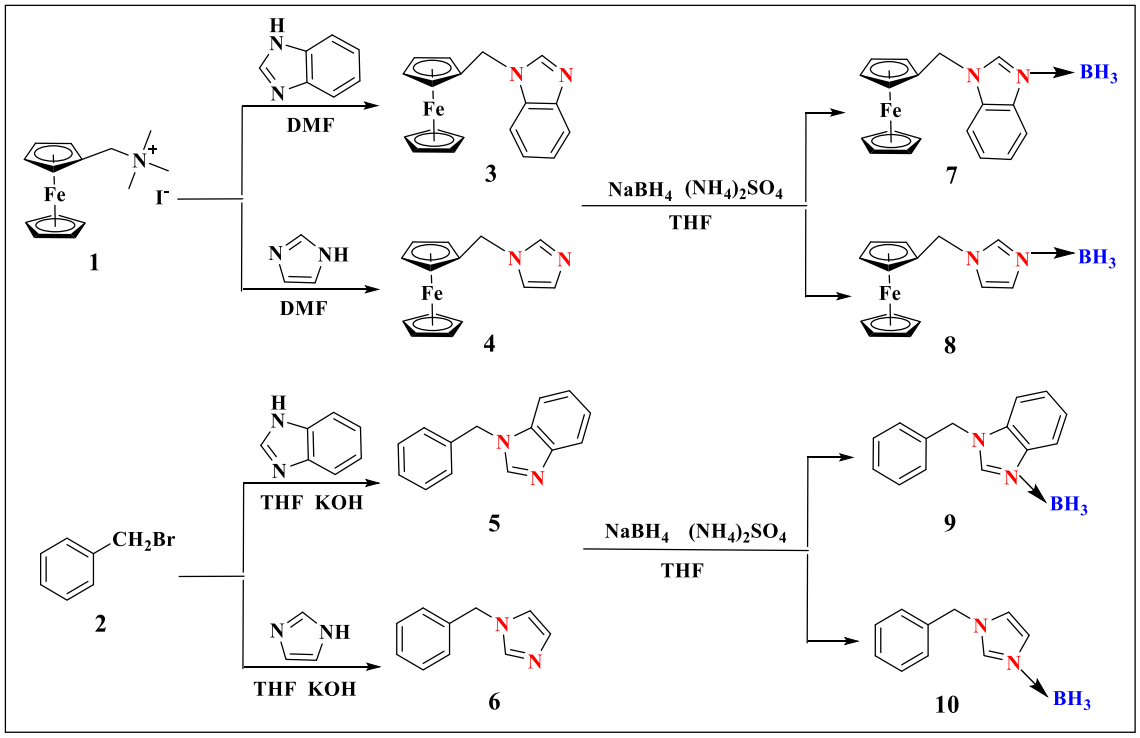

Scheme 1. Synthetic procedure of compounds **7-10**.

Table 1
Crystal data and structure refinement for **7, 8, 9**.

Compound	7	8	9
Chemical formula	$C_{18}H_{19}BFeN_2$	$C_{14}H_{17}BFeN_2$	$C_{14}H_{15}BN_2$
Formula weight	330.01	279.96	222.13
Temperature (K)	296(2)	296(2)	296(2)
Crystal system	Monoclinic	Monoclinic	Monoclinic
Space group	$P2_12_12_1$	$P2_12_12_1$	$P2_1/c$
a (Å)	8.2008(14)	10.0167(7)	9.4606(5)
b (Å)	9.9847(15)	11.4232(7)	15.4485(8)
c (Å)	19.067(3)	11.7815(8)	8.5232(4)
α (°)	90.00	90.00	90.00
β (°)	90.00	90.00	98.003(2)
γ (°)	90.00	90.00	90.00
V (Å^3)	1561.2(4)	1348.07(16)	1233.55(11)
Z	4	4	26
Crystal size(mm^3)	0.50 × 0.40 × 0.20	0.50 × 0.40 × 0.20	0.50 × 0.40 × 0.20
D_c (mg m^{-3})	1.404	1.379	1.196
Abs coeff (mm^{-1})	0.962	1.100	0.070
F(000)	688	584	472
θ range (°)	2.30-25.03	2.48 -25.02	2.17-25.03
Reflections collected	5886	16044	19800
Independent reflections	2706	2374	2176
Goodness-of-fit on F^2	1.055	1.051	1.092
$R_{(int)}$	0.0355	0.0671	0.0480
R1/wR_2[$I > 2\sigma(I)$]	0.0323/0.0543	0.0271/0.0536	0.0394/0.0913
R1/wR_2 (all data)	0.0403/0.0562	0.0335/0.0554	0.0508/0.0972

The single crystal structures of compounds **7-9** were illustrated in Fig. 1. In order to facilitate the description of the hydrogen atoms on the boron, the whole single crystal structures didn't shield the hydrogen atoms. In the single crystal structure of compound **7**, two cyclopentadiene (Cp) rings of a ferrocenyl group were nearly eclipsed. The angle between the substituted Cp ring (Cp ring: C6-C10) plane of ferrocenyl moieties with the benzimidazolium ring was 71.06° (Fig. 1a), owing to a free methylene group between them. There were not intermolecular π-π interaction or hydrogen bonding in **7**. In addition, there was only a {BH3} not a borane dimer, which can be supported by ^{11}B NMR (Fig. S3). The boron spectra of the four compounds were split into quartet or re-folded doublet with hydrogen coupling. The {BH_3} moiety was coordinated with N(2) atom in the benzimidazolium framework. The length of N(2)-B(1) was 1.579 Å and the bond angles of C12-N2-B1 and C13-N2-B1 bonds were up to 127.4(3)°and 126.2(3)°, respectively, which was consistent with the bond length (1.579 Å) of the nitrogen-boron coordination bond in a similar structure reported in the literature [17]. The single crystal structures of compounds **8** and **9** were similar to **7**. It was worth pointing out that the angle between the substituted Cp ring and the imidazole ring in the single crystal structure of compound **8** was 66.08° (Fig. 1b) and the

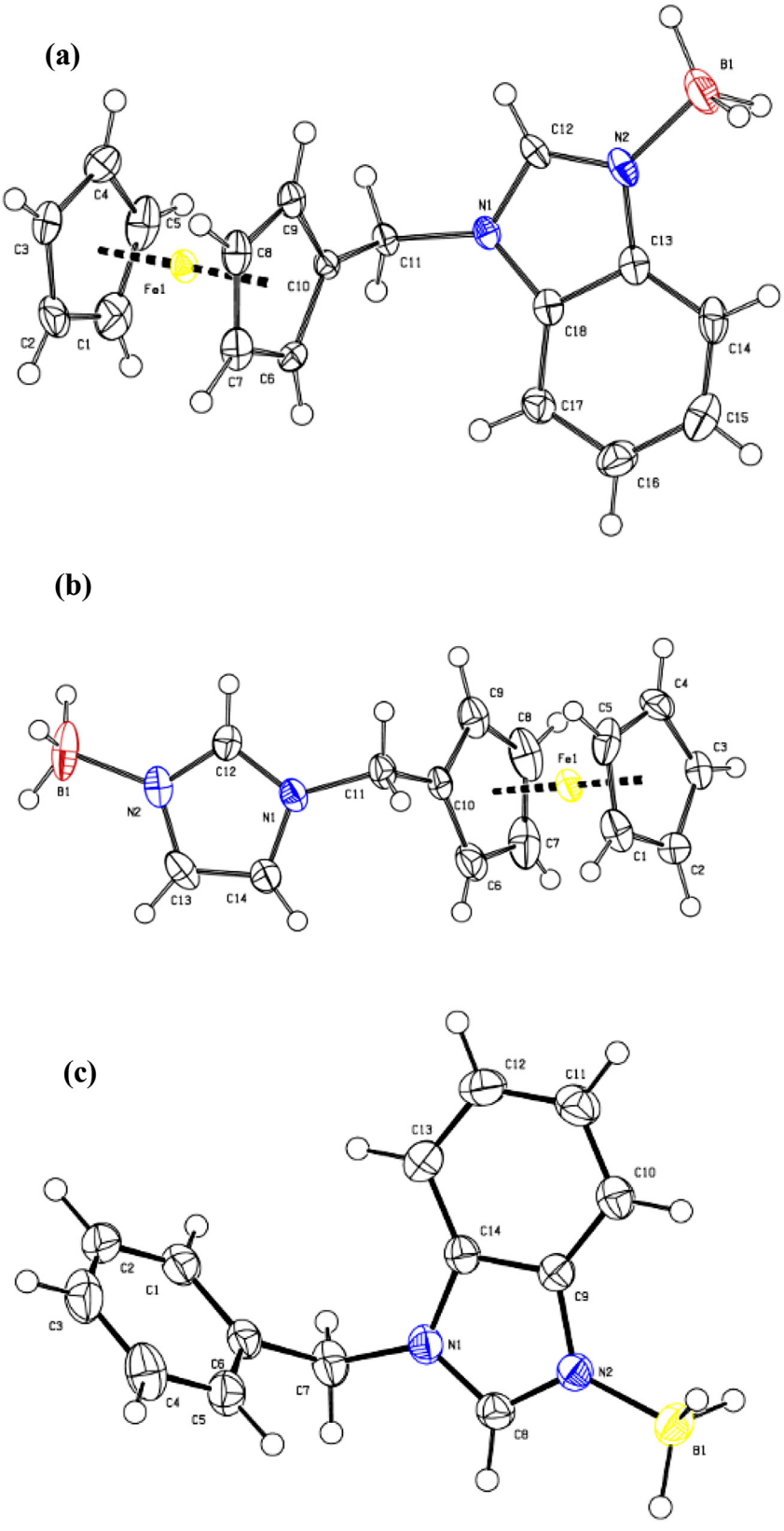

Fig. 1. Molecular structures of (a) **7**, (b) **8**, (c) **9** (thermal ellipsoids were set at 50 % probability).

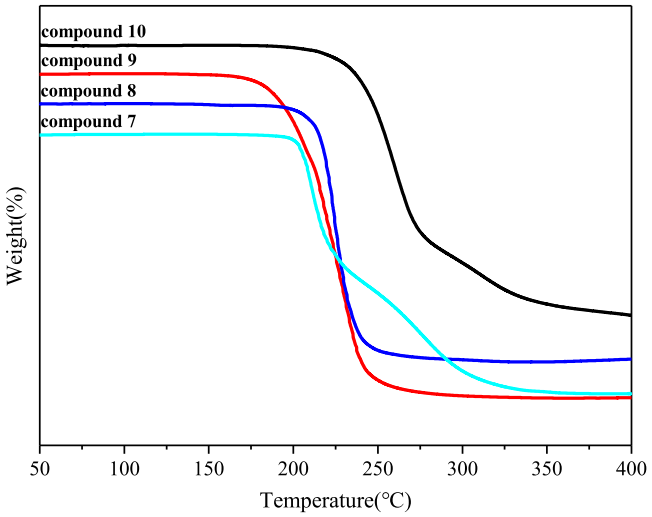

Fig. 2. TG curve of compounds **7-10**.

Table 2
Thermal properties of borane compounds **7-10**.

Compound	7	8	9	10
T_m /°C	189-190	163-164	131-132	93-94
T_d /°C	210	222	182	256
W_{ls} /%	70.8	70.7	89.1	73.4

[a] T_m: melting point; [b] T_d: thermal decomposition temperature; [c] W_{ls}: weightlessness ratio.

angle between the benzene ring and the benzimidazole ring in the single crystal structure of compound **9** was 79.02° (Fig. 1c).

2.3. Thermal stability of compounds *7-10*

As shown in Fig. 2, compounds **7-10** showed no obvious weightlessness at the beginning. As the temperature continued to rise, the structures of compounds collapsed and they began to lose weight quickly. The specific decomposition temperatures and weightlessness ratios of four compounds were shown in Table 2. The decomposition temperatures of compounds **7-10** were ranged from 182 to 256°C. Ferrocene-based derivatives (**7** and **8**) had lower weightlessness ratios than benzene-based derivatives (**9** and **10**), which may be due to the conversion of ferrocene into ferric oxide at high temperature [20,21]. In addition, compounds **8** and **10** containing imidazolyl were more stable than compounds **7** and **9** containing benzimidazolyl from the perspective of the decomposition temperatures. Based on the TG curves and the melting points, the compounds had a liquefaction process. Among them, compound **10** showed the best stability with the widest temperature range (94-256 °C) in the liquid state. Ferrocene-based derivatives (**7** and **8**) also had high thermal stability, but the stable temperature range of them in the liquid state was shorter than that of compound **10**.

2.3. Combustion test

To verify the reduction and combustion behavior of the compounds, ignition tests were conducted according reported procedures [32,33]. Each sample (about 10 mg) was dropped into a 10 mL glass beaker containing concentrated HNO_3 (2 mL) and recorded with a 1000 fps high-speed camera at the same time. Visual analysis of four compounds showed that all compounds could burn rapidly with high flame height. A series of images of compound 8 collected with the high-speed camera were shown in

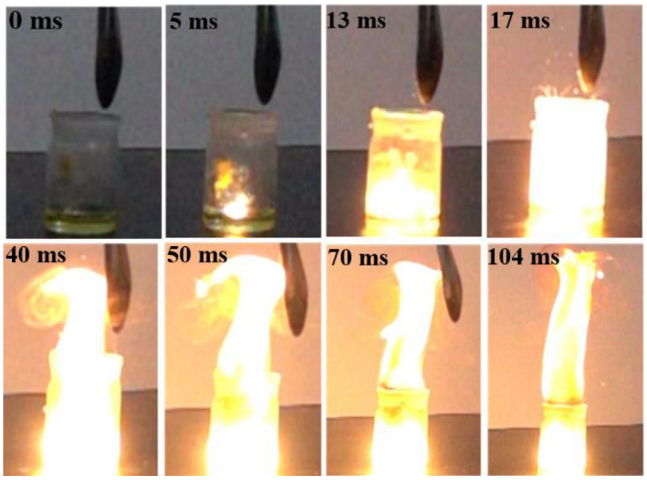

Fig. 3. Combustion changes of compound **8** under concentrated HNO_3 at different times.

Table 3
Ignition time (T_i) of borane compounds **7-10**.

Compound	7	8	9	10
T_i /ms	7	5	37	67

Fig. 3 as an example. The ignition time (T_i) of compounds **7-10** were collected in Table 3. It could be found that compounds **7** and **8** with ferrocenyl groups took less time than compounds **9** and **10** to start combustion with concentrated HNO_3 and compound **8** was ignited in the shortest time (5 ms). The ferrocene-containing stereo aromatic structure may play a role in accelerating combustion. Moreover, intermediate **4** without $\{BH_3\}$ moiety couldn't be ignited when the same operation was performed. It can be speculated that the vigorous combustion of compound was result from a violent oxidation-reduction stimulated by the B-H bonds in compound with the oxidant HNO_3. However, if the HNO_3 was dripped onto compounds **7-10** with burettes, the phenomenon shown in the Fig. 3 couldn't be observed, which was caused by the insufficient contact between HNO_3 and products. Besides, the concentration of HNO_3 had a great influence on the ignition experiment, that HNO_3 with a concentration lower than 95% couldn't ignite the compounds.

2.4. Catalytic effect on the decomposition of ammonium perchlorate (AP)

Ferrocene derivatives are widely used catalysts and their potential as propellants can usually be estimated by studying their catalytic effects on AP [1]. The catalytic effects of the products on AP were evaluated used TG analysis with a weight percentage of BRCs in AP were generally 2–5 wt.% [5,26]. Hence, we prepared four samples of pure AP and mixtures of AP with 2 wt.%, 3 wt.%, 5 wt.% of compound **7** and compared their thermal decomposition process by TG. As shown in Fig. 4, the final thermal decomposition temperature of AP was 443 °C. After adding 2 wt.%, 3 wt.%, 5 wt.% of compound **7**, the final thermal decomposition temperatures of AP decreased by 42 °C, 52 °C, 65 °C, respectively. Furthermore, TG curves of pure AP and mixtures of AP with 5 wt.% of four products were investigated. As illustrated in Fig. 5, with the addition of **7** and **8** the final thermal decomposition temperatures of AP decreased to 378 °C and 398 °C, while with the addition of **9** and **10**, the final thermal decomposition temperatures only reduced to 411 °C and 419 °C, which indicated that benzene-based

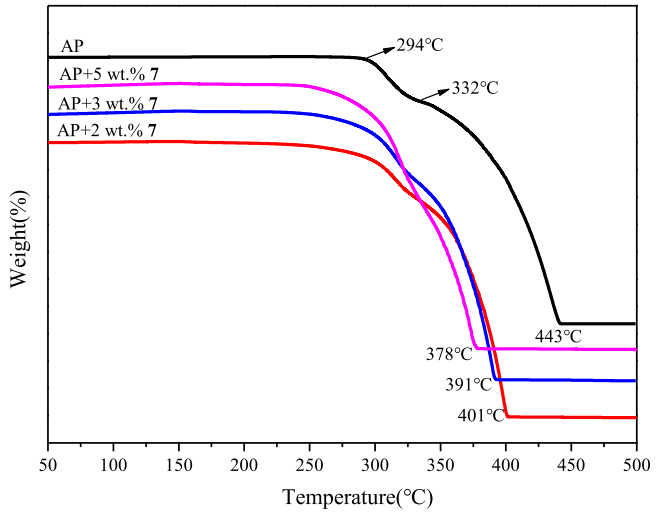

Fig. 4. TG curve of AP, AP + 2 wt.% **7**, AP + 3 wt.% **7**, AP + 5 wt.% **7**.

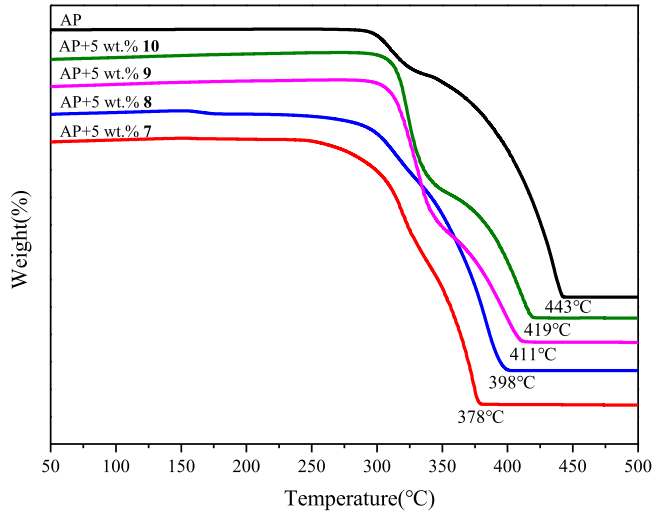

Fig. 5. TG curve of AP, AP + 5 wt.% compound (**7**-**10**).

derivatives **9** and **10** had poorer catalytic effects on AP compared with ferrocenyl-based derivatives **7** and **8**. However, the effect of benzimidazole or imidazole groups in compound on the catalytic thermal decomposition of AP was not obvious.

Specifically, researchers generally agreed that the thermal decomposition of AP was divided into two parts as shown in Fig. 4. Firstly, AP would decompose to produce NH_3 and $HClO_4$ at the lower temperature (294 °C - 332 °C). Then NH_3 would adhere to the surface of AP and $HClO_4$ further decomposed to produce various oxidizing products. Secondly, as NH_3 desorbed on the surface of AP at the higher temperature (332 °C - 443 °C), AP continued to react and decompose. [27,28]. As mentioned above, the decomposition temperatures of four additives (**7**-**10**) were all below 256 °C (Table 2), which was much lower than the thermal decomposition temperature of AP. And compounds **7**-**10** released a certain amount of hydrogen when they decomposed [29,30]. Hydrogen reacted with the oxidizing products produced by $HClO_4$, which would further increase the reaction rate of $HClO_4$. We can find evidence to support the above view from Fig. 5. After adding additives **9** and **10**, TG curve of AP would lose weight quickly in the first part compared with the thermal decomposition of pure AP. Therefore, the thermal decomposition process of AP proceeded in the atmosphere of some hydrogen, which gave out heat and accelerated the decomposition of AP. Consequently, we can explain why the benzene-based derivatives (**9** and **10**) had catalytic effects on AP. We believed that the catalytic effects of **7** and **8** on AP also benefited from B-H bonds. But due to the influence of ferrocene, the weight loss of AP in the first process was not obvious, especially after increasing the content of ferrocene derivatives as shown in Fig. 4.

3. Conclusion

In this paper, we have synthesized four energetic small molecular compounds, *N*-(arylmethylene)- benzimidazole/imidazole-borane compounds (**7-10**) with relatively cheap raw materials $NaBH_4$ and $(NH_4)_2SO_4$. These products possessed some unique properties including the high stability, outstanding ignition performance with HNO_3 and catalytic effect for AP. Ferrocene-based derivatives (**7** and **8**) took less times than benzene-based derivatives (**9** and **10**) to start combustion with HNO_3. Compounds **7**-**10** all had catalytic effects on AP as burning rate catalysts in propellants. Compound **7** had the best catalytic effect on AP with the final thermal decomposition temperature of AP decreased to 378 °C. In summary, we believed that ferrocene-based derivatives (**7** and **8**) had good ignition and combustion-supporting performance at once and would have great value in propellants.

4. Experimental

4.1. General methods

All chemicals were commercially available. All reactions were performed under an atmosphere of dry nitrogen. Melting points (M.p.) were determined with a 4 × micro melting point apparatus. Nuclear magnetic resonance spectra (^1H and ^{13}C and ^{11}B NMR) were measured in $CDCl_3$, with tetramethylsilane (TMS) as the internal standard, with a Bruker AV400 spectrometer at ambient temperature. High resolution mass spectrometer was obtained on an Accurate-Mass Q-TOFLC/MS. The intermediate 1-(ferrocenylmethyl)benzimidazole (**3**) [22], 1-(ferrocenylmethyl)imidazole (**4**) [23], 1-(benzyl)benzimidazole (**5**) [24], 1-(benzyl)imidazole (**6**) [24] were synthesized by the procedures according to the literatures.

X-ray structural measurements were carried out on a Rigaku RAXISIV CCD diffract meter with a graphite-monochromator Mo Kα radiation (λ = 0.071073 nm) at 296(2) K. All diffraction data were collected by scanning in a certain mode and refined in Lp factor. All data were corrected by semi-empirical method using SADABS program, the SAINT program was used for integration of the diffraction profiles. The structure was solved by the direct methods using SHELXS program of the SHELXL-97 [31]. The position coordinates and each anisotropic thermal parameter of nonhydrogen atoms were refined by full-matrix least-squares on F2 through confirmation. All hydrogen atoms were generated geometrically assigned appropriated isotropic thermal parameters and included in the final calculations.

Thermogravimetry (TG) analysis on compounds **7-10** and AP were dried under 0.1 MPa at 20 °C, then recorded with a TG Thermal Analyzer SDT Q600 instrument. The experiments were conducted at heating rate of 10 °C/min.

4.2. General procedure for compounds **7-10**

4.2.1. Synthesis of *N*-(ferrocenylmethyl)-benzimidazole- borane (**7**)

A solution of $NaBH_4$ (114 mg, 3 mmol) and $(NH_4)_2SO_4$ (198 mg, 1.5 mmol) was added to THF (5 mL) under vigorous stirring. 1-(ferrocenylmethyl)benzimidazole (100 mg, 0.30 mmol,) which was dissolved with THF (30 mL) was added dropwise to the reaction

system and refluxed at 66°C for 0.5 h. After cooling to room temperature, the mixture was filtered with diatomite and washed with dichloromethane. The residue was purified by column chromatography to give compound as a yellow solid. Yield 93.3 % (94 mg). M.p. 189-190 °C. ^{1}H NMR (400 MHz, Chloroform-*d*) δ: 8.05 (s, 1H, NCHN), 8.00 – 7.94 (m, 1H, PhH), 7.56 – 7.50 (m, 1H, PhH), 7.46 (t, *J*= 7.1 Hz, 2H, PhH), 5.12 (s, 2H, CH_2), 4.29 (s, 2H, CpH), 4.28 (s, 2H, CpH), 4.24 (s, 5H, CpH), 2.64 – 2.10 (m, 3H, BH_3). ^{13}C NMR (101 MHz, Chloroform-*d*) δ: 141.03, 137.37, 132.20, 124.94, 124.73, 117.63, 110.52, 70.06, 69.66, 69.33, 69.03, 45.99. ^{11}B NMR (128 MHz, Chloroform-*d*) δ: -21.32 (q, J_{BH} = 91.7 Hz). HRMS (ESI$^+$): $C_{18}H_{19}BFeN_2$, $[M+Na]^+$ requires 353.0883, found 353.0877.

*4.2.2. Synthesis of N-(ferrocenylmethyl)-imidazole- borane (**8**)*

Compound **8** was prepared by adopting the same procedure as that of **7** by using $NaBH_4$ (137 mg, 3.60 mmol) and $(NH_4)_2SO_4$ (238 mg, 1.8 mmol) and 1-(ferrocenylmethyl)imidazole (100 mg, 0.36 mmol). The pure product obtained was a yellow solid. Yield 77.5 % (87.7 mg). M.p.163-164 °C. ^{1}H NMR (400 MHz, Chloroform-*d*) δ: 7.67 (s, 1H, NCHN), 7.01 (s, 1H, NCH), 6.85 (s, 1H, NCH), 4.88 (s, 2H, CH_2), 4.25 (m, 2H, CpH), 4.23 (m, 2H, CpH), 4.19 (s, 5H, CpH), 2.48 – 1.92 (m, 3H, BH_3). ^{13}C NMR (101 MHz, Chloroform-*d*) δ: 135.61, 127.57, 119.38, 79.58, 69.59, 69.03, 68.96, 48.39. ^{11}B NMR (128 MHz, Chloroform-*d*) δ: -19.47 (q, J_{BH}= 92.7 Hz). HRMS (ESI$^+$): $C_{14}H_{17}BFeN_2$, $[M+Na]^+$ requires 303.0726, found 303.0723.

*4.2.3. Synthesis of N-(benzyl)-benzimidazole -borane (**9**)*

Compound **9** was prepared in a manner analogous to that of **7** by using $NaBH_4$ (171 mg, 4.50 mmol) and $(NH_4)_2SO_4$ (297 mg, 2.25 mmol) and 1-(benzyl)benzimidazole (100 mg, 0.45 mmol). The pure product obtained was a white solid. Yield 83.8 % (89.5 mg). M.p.131-132 °C. ^{1}H NMR (400 MHz, Chloroform-*d*) δ: 8.17 (s, 1H, NCHN), 7.98 (d, *J*= 8.0 Hz, 1H, PhH), 7.52 – 7.34 (m, 6H, PhH), 7.26 – 7.19 (m, 2H, PhH), 5.37 (s, 2H, CH_2), 2.78 – 1.99 (m, 3H, BH_3).^{13}C NMR (101 MHz, Chloroform-*d*) δ: 141.72, 137.49, 133.18, 132.44, 129.44, 129.18, 127.76, 125.23, 124.88, 117.65, 110.92, 49.98. ^{11}B NMR (128 MHz, Chloroform-*d*) δ: -21.10 (q, J_{BH} = 90.3 Hz). HRMS (ESI$^+$): $C_{14}H_{15}BN_2$, $[M+Na]^+$ requires 245.1221, found 245.1217.

*4.2.4. Synthesis of N-(benzyl)-imidazole -borane (**10**)*

The procedure adopted for the preparation of **10** the same as that of **7** using $NaBH_4$ (221 mg, 5.80 mmol) and $(NH_4)_2SO_4$ (383 mg, 2.90 mmol) and 1-(benzyl)imidazole (100 mg, 0.58 mmol). The pure product obtained was a white solid. Yield 81.3 % (87.8 mg). M.p.93-94 °C. ^{1}H NMR (400 MHz, Chloroform-*d*) δ: 7.76 (s, 1H, NCHN), 7.43 – 7.35 (m, 3H, PhH), 7.24 – 7.17 (m, 2H, PhH), 7.06 (s, 1H, NCH), 6.89 (s, 1H, NCH), 5.11 (s, 2H, CH_2), 2.63 – 1.90 (m, 3H, BH_3).^{13}C NMR (101 MHz, Chloroform-*d*) δ:136.36, 133.64, 129.41, 129.23, 128.01, 52.32. ^{11}B NMR (128 MHz, Chloroform-*d*) δ: -19.32 (q, J_{BH} = 91.2 Hz). HRMS (ESI$^+$): $C_{10}H_{13}BN_2$, $[M+Na]^+$ requires 195.1064, found 195.1062.

Declaration of Competing Interest

None.

Acknowledgements

This work was supported financially by the National Natural Science Foundation of China (No. 21642009 and 21772023) and the Valuable Instrument and Equipment Open Test Fund of Fuzhou University (No. 2019T004). We also thank You-Ren Huang for his help in crystal analysis.

Appendix A. Supplementary material

^{1}H NMR, ^{13}C NMR and ^{11}B NMR of compounds **7-10** were given in Figs. S1-S12. HRMS spectra of compounds **7-10** were given in Figs. S13-S16. Selected bond lengths (Å) and angles for compounds **7-9** were given in Tables S1-S6. CCDC 1978238, 1978239 and 1978240 contained the supplementary crystallographic data for this paper. These data can be obtained free of charge from The Cambridge Crystallographic Data Centre via www.ccdc.cam.ac.uk/data_request/cif.

Supplementary materials

Supplementary material associated with this article can be found, in the online version, at doi:10.1016/j.jorganchem.2020.121544.

References

[1] M. Usman, L. Wang, H.J. Yu, F. Haq, M. Haroon, R.S. Ullah, A. Khan, S. Fahad, A. Nazir, T. Elshaarani, J. Organomet. Chem. 872 (2018) 40–53.
[2] R.B. Tong, Y.L. Zhao, L. Wang, H.J. Yu, F.J. Ren, M. Saleem, W.A. Amer, J. Organomet. Chem. 755 (2014) 16–32.
[3] Y. Gao, H.D. Li, C.F. Ke, L.L. Xie, B. Wei, Y.F. Yuan, Appl. Organomet. Chem. 25 (2011) 407–411.
[4] J.B. Zhuo, H.D. Li, C.X. Lin, L.L. Xie, S. Bai, Y.F. Yuan, J. Mol. Struct. 1067 (2014) 112–119.
[5] Z.M. Lai, H.M. Ye, Q. Wan, L.L. Xie, S. Bai, Y.F. Yuan, J. Mol. Struct. 1059 (2014) 33–39.
[6] A. Zainul, L. Wang, H. Yu, M. Saleem, M. Akram, H. Khalid, N.M. Abbasi, R.U. Khan, Appl. Organomet. Chem. 31 (2017) 3754.
[7] X. Liu, J. Li, F. Bi, W. Zhang, G. Zhang, Z. Gao, Eur. J. Inorg. Chem. 2015 (2015) 1496–1504.
[8] K.F. Grythe, F.K. Hansen, J. Appl. Polym. Sci. 103 (3) (2007) 1529–1538.
[9] F.-W. Grevels, A. Kuran, S. Özkar, M. Zora, J. Organomet. Chem. 587 (1999) 122–126.
[10] Z. Deng, H. Yu, L. Wang, X. Zhai, Y. Chen, R. Sun, J. Organomet. Chem. 799 (2015) 273–280.
[11] X. Liu, D. Zhao, F. Bi, X. Fan, F. Zhao, G. Zhang, W. Zhang, Z. Gao, J. Organomet. Chem. 762 (2014) 1–8.
[12] J.B. Zhuo, Z.H. Ma, C.X. Lin, L.L. Xie, S. Bai, Y.F. Yuan, J. Mol. Struct. 1085 (2015) 13–20.
[13] S. Huang, X.J. Qi, T.L. Liu, K.C. Wang, W.Q. Zhang, J.L. Li, Q.H. Zhang, Chem. Eur. J. 22 (2016) 10187–10193.
[14] Q.H. Zhang, P. Yin, J.H. Zhang, J.M. Shreeve, Chem. Eur. J. 20 (2014) 6909–6914.
[15] Y.H. Jin, B.S. Wang, W.Q. Zhang, S. Huang, K.C. Wang, X.J. Qi, Q.H. Zhang, Chem. Eur. J. 24 (2018) 4620–4627.
[16] T.L. Liu, X.J. Qi, S. Huang, L.H. Jiang, J.L. Li, C.L. Tang, Q.H. Zhang, Chem. Commun. 52 (2016) 2031–2034.
[17] S. Huang, W.Q. Zhang, T.L. Liu, K.C. Wang, X.J. Qi, J.H. Zhang, Q.H. Zhang, Chem. Asian J. 11 (24) (2016) 3528–3533.
[18] S. Huang, X.J. Qi, W.Q. Zhang, T.L. Liu, Q.H. Zhang, Chem. Asian J. 10 (2015) 2725–2732.
[19] Q.H. Zhang, J.M. Shreeve, Chem. Rev. 114 (2014) 10527–10574.
[20] R.L. Sun, L. Wang, H.J. Yu, A. Zain-ul, Y.S. Chen, H. Khalid, N. Abbasi, M. Akram, J. Inorg. Organomet. Polym. 24 (2014) 1063–1069.
[21] Z. Deng, H.J. Yu, L. Wang, X.T. Zhai, Y.S. Chen, R.L. Sun, J. Organomet. Chem. 771 (2015) 273–280.
[22] J.B. Zhuo, X.X. Zhu, C.X. Lin, S. Bai, L.L. Xie, Y.F. Yuan, J. Organomet. Chem. 770 (2014) 85–93.
[23] V. Bui-Thi-Tuyet, G. Trippe-Allard, J. Ghilane, H. Randriamahazaka, ACS Appl. Mater. Interfaces 8 (2016) 28316–28324.
[24] R.M. Cywar, L. Wang, E.Y-X. Chen, ACS Sustain. Chem. Eng. 7 (2019) 1980–1988.
[25] I.I. Padilla-Martinez, F.J. Martinez-Martinez, A. Lopez-Sandoval, K.I. Giron–Castillo, M.A. Brito, R. Contreras, Eur. J. Inorg. Chem. 10 (1998) 1547–1553.
[26] H.Y. Zhao, X.Y. Zhu, Y.D. Shang, S.F. Chen, B.G. Li, Z.X. Bian, RSC Adv. 6 (2016) 34476–34483.
[27] P.W.M. Jacobs, G.S. Pearson, Combust. Flame 13 (1969) 419–430.
[28] W.A. Rosser, S.H. Inami, H. Wise, Combust. Flame 12 (1968) 427–435.
[29] G.P. Rachiero, H.M. Titi, R.D. Rogers, Chem. Commun. 53 (2017) 7736–7739.
[30] A.S. Rozenberg, G.N. Nechiporenko, A.P. Alekseev, Russ. Chem. Bull. 27 (1978) 284–287.
[31] G.M. Sheldrick, Acta Crystallogr. Sect. A 64 (2008) 112–122.
[32] B. Wu, Y. Lai, X.F. Qi, H.Y. Du, C.H. Pei, ACS Appl. Energy Mater. 2 (2019) 8319–8327.
[33] H.X. Gao, J.M. Shreeve, Chem. Rev. 111 (2011) 7377–7436.